

Cluster Condensation by Thermolysis: Synthesis of a Rhomb-Linked $\text{Re}_{12}\text{Se}_{16}$ Dicluster and Factors Relevant to the Formation of the $\text{Re}_{24}\text{Se}_{32}$ Tetracluster

Zhiping Zheng and R. H. Holm*

Department of Chemistry and Chemical Biology, Harvard University, Cambridge, Massachusetts 02138

Received June 12, 1997[©]

The cluster $\text{cis-}[\text{Re}_6\text{Se}_8(\text{PET}_3)_4\text{L}_2]$ undergoes substitution reactions with neutral ligands L in the presence of AgSbF_6 to afford the cis- disubstituted clusters $[\text{Re}_6\text{Se}_8(\text{PET}_3)_4\text{L}_2]^{2+}$ (L = MeCN (**6**), *t*-BuCN, DMF, Me_2SO (**9**)). Cluster **6** reacts with pyridine to give $[\text{Re}_6\text{Se}_8(\text{PET}_3)_4(\text{py})_2]^{2+}$. Retention of stereochemistry was demonstrated from ^{31}P NMR spectra and the crystal structure of **9**(SbF₆)₂, which revealed the two Me_2SO ligands to be O-bonded at adjacent Re sites of the face-capped octahedral $[\text{Re}_6(\mu_3\text{-Se})_8]^{2+}$ core. The clusters $\text{cis-}[\text{Re}_6\text{Se}_8(\text{PET}_3)_4\text{L}_2]^{2+}$ are of interest as possible precursors to oligomeric clusters under thermolysis conditions where one or both ligands L are removed. Thermolysis of orange-red **6**(SbF₆)₂ (180 °C, 24 h) afforded a brown-green crystalline product identified by an X-ray structure determination to contain the dicluster $[\text{Re}_{12}\text{Se}_{16}(\text{PET}_3)_8(\text{MeCN})_2]^{4+}$ (**11**). Two $[\text{Re}_6\text{Se}_8]^{2+}$ cluster units are bridged by a Re_2Se_2 rhomb to afford the centrosymmetric core $[\text{Re}_{12}(\mu_3\text{-Se})_{14}(\mu_4\text{-Se})_2]^{4+}$, established recently for the dicluster $[\text{Re}_{12}\text{Se}_{16}(\text{PET}_3)_{10}]^{4+}$. The two acetonitrile ligands occur in a *trans* orientation on the two cluster units. From consideration of the crystal structure of the precursor compound **6**(SbF₆)₂ (reported earlier), the relative orientation of cluster pairs could be responsible for the formation of *trans*-**11**. Diclusters of the type $\text{cis-}[\text{Re}_{12}\text{Se}_{16}(\text{PET}_3)_8\text{L}_2]^{4+}$ are required for potential thermolytic conversion to the cyclic tetracluster $[\text{Re}_{24}\text{Se}_{32}(\text{PET}_3)_{16}]^{8+}$. Factors relevant to the formation of this unknown cluster type are considered.

Introduction

Under our previous classification scheme for metal chalcogenide/halide solids,¹ the compounds $\text{Re}_6\text{Q}_8\text{X}_2$ (Q = S,^{2,3} Se;^{3–5} X = halide) are type III solids because they contain discrete, recognizable clusters, independent except for the bridging interactions between them. Consequently, they serve as sources of clusters possessing the face-capped octahedral, electron-precise $[\text{Re}_6(\mu_3\text{-Q})_8]^{2+}$ cores. In previous investigations,^{6,7} we demonstrated that the decidedly stable two- and three-dimensional frameworks of these compounds can be dismantled by high-temperature reactions with M^+X ($\text{M}^+ = \text{Cs}^+, \text{TI}^+$). Each equivalent of the latter severs one bridging interaction between clusters, with the final result being a solid phase containing the individual cluster anions $[\text{Re}_6\text{Q}_8\text{X}_6]^{4-}$. In this way, clusters locked in intractable solids can be rendered in molecular form for further investigation.⁸ The process by which a lattice is deconstructed to afford, ultimately, a molecular solid is termed dimensional reduction, a concept of some generality in reducing the connectedness of polymeric solids.

The halide ligands of $[\text{Re}_6\text{Q}_8\text{X}_6]^{4-}$ are replaceable by triethylphosphine in direct reactions, leading to the cluster sets

$[\text{Re}_6\text{Se}_8(\text{PET}_3)_n\text{I}_{6-n}]^{(n-4)+}$ ($n = 3-6$)⁹ and $[\text{Re}_6\text{S}_8(\text{PET}_3)_n\text{Br}_{6-n}]^{(n-4)+}$ ($n = 2-6$).¹⁰ Nearly all isomers of these species have been isolated and structurally characterized by NMR and X-ray crystallography. Further, in the presence of a silver(I) salt, halide may be substituted by solvent ligands to afford clusters such as $[\text{Re}_6\text{Se}_8(\text{PET}_3)_5(\text{MeCN})]^{2+}$, $\text{cis-}[\text{Re}_6\text{Se}_8(\text{PET}_3)_4(\text{MeCN})_2]^{2+}$, and fully solvated $[\text{Re}_6\text{Se}_8(\text{MeCN})_6]^{2+}$.⁹ Clusters with relatively labile solvent ligands can act as precursors to other species, allowing an extensive family of differently substituted $[\text{Re}_6\text{Se}_8]^{2+}$ clusters. Another reactivity feature of these clusters is described in Figure 1. In reaction 1, monosubstituted cluster **1** releases solvent ligand L upon heating, affording an intermediate which alleviates its single-site coordinative unsaturation by condensing with another such species to yield the dicluster **2**. In the example shown, individual clusters are connected by means of an Re_2Se_2 rhomb, the same interaction that links clusters in the two-dimensional structure of $\text{Re}_6\text{Se}_8\text{Cl}_2$ ($[\text{Re}_6\text{Se}_4^i\text{Se}^{-i}_{4/2}\text{Se}^{-i}_{4/2}\text{Cl}^a_2]$).⁴ The cluster condensation concept is potentially extendable in the form of reaction 2. Here, the cis- disubstituted cluster **3** is deligated to a doubly unsaturated intermediate which condenses with another to form the cyclic tetracluster **4** having four connecting rhombs. Other variations on this theme are conceivable, including, for example, the conversion of $\text{trans-}[\text{Re}_6\text{Se}_8(\text{PR}_3)_4\text{L}_2]^{2+}$ to the linear polymer $[\text{Re}_6\text{Se}_8(\text{PET}_4)]_n^{2n+}$.

We are attracted to the transformations illustrated in Figure 1 as a means of directed synthesis of bridged multicluster assemblies, an essentially unknown class of molecular clusters at the supramolecular level of complexity. Thermolysis of cluster **1** has only one conceivable outcome, provided L is more labile than PR_3 . In this circumstance, the phosphine ligands serve as protecting groups for their coordinated rhenium atoms. Recently, we demonstrated the occurrence of reaction 1 by

[©] Abstract published in *Advance ACS Abstracts*, October 15, 1997.

- Lee, S. C.; Holm, R. H. *Angew. Chem., Int. Ed. Engl.* **1990**, *29*, 840.
- Fischer, C.; Fiechter, S.; Tributsch, H.; Reck, G.; Schultz, B. *Ber. Bunsen-Ges. Phys. Chem.* **1992**, *96*, 1652.
- Fischer, C.; Alonso-Vante, N.; Fiechter, S.; Tributsch, H.; Reck, G.; Schulz, W. *J. Alloys Compd.* **1992**, *178*, 305.
- (a) Leduc, P. L.; Perrin, A.; Sergent, M. *Acta Crystallogr.* **1983**, *C39*, 1503. (b) Leduc, L.; Padiou, J.; Sergent, M. *J. Less-Common Met.* **1983**, *95*, 73.
- Spezial, N. L.; Berger, H.; Leicht, G.; Sanjinés, R.; Chapius, G.; Lévy, F. *Mater. Res. Bull.* **1988**, *23*, 1597.
- Long, J. R.; Williamson, A. S.; Holm, R. H. *Angew. Chem., Int. Ed. Engl.* **1995**, *34*, 226.
- Long, J. R.; McCarty, L. S.; Holm, R. H. *J. Am. Chem. Soc.* **1996**, *118*, 4603.
- Recently, the compound $\text{Cs}_4\text{KRe}_6\text{S}_8\text{Br}_7$ was prepared by solid state synthesis and shown to contain the $[\text{Re}_6\text{S}_8\text{Br}_6]^{4-}$ cluster: Slogui, A.; Ferron, S.; Perrin, A.; Sergent, M. *Eur. J. Solid State Chem.* **1996**, *33*, 1001.

(9) Zheng, Z.; Long, J. R.; Holm, R. H. *J. Am. Chem. Soc.* **1997**, *119*, 2163.

(10) Willer, M. W.; Long, J. R.; McLauchlan, C. C.; Holm, R. H. Results to be published.

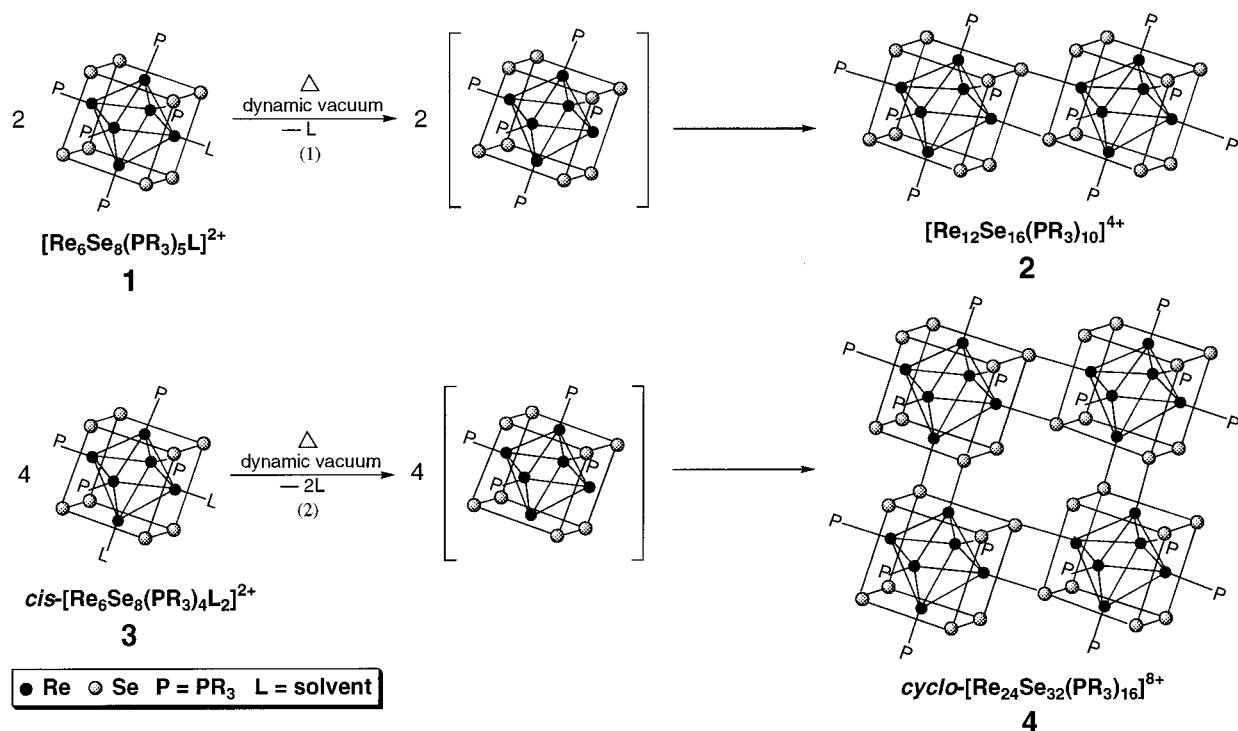


Figure 1. Directed synthesis of dicluster **2** from monocluster **1** containing one labile ligand (reaction 1) and of tetracluster **4** from monocluster **3** containing labile ligands in *cis* positions (reaction 2).

thermolytic conversion of $[\text{Re}_6\text{Se}_8(\text{PET}_3)_5(\text{MeCN})]^{2+}$ to $[\text{Re}_{12}\text{Se}_{16}(\text{PET}_3)_{10}]^{4+}$, whose structure **2** was proven by crystallography.⁹ In the course of this work, we observed that the orientation of clusters in a crystal of $[\text{Re}_6\text{Se}_8(\text{PET}_3)_5(\text{MeCN})](\text{BF}_4)_2$, with solvated sites in pairs of clusters facing each other, is decidedly propitious for dicluster formation. With this result in hand, we have turned to an examination of reaction 2 as a means of achieving the unknown tetracluster **4**. The results from our initial examination of this reaction type are described here.

Experimental Section

Preparation of Compounds. Standard Schlenk and vacuum-line techniques were employed for all manipulations of dioxygen- and/or moisture-sensitive compounds. Solvents were distilled from appropriate drying agents and degassed prior to use. Reagents were of commercial origin and were used as received. NMR spectra of all compounds were determined in CD_3CN solution; proton spectra were not ^{31}P -decoupled (q = quartet, quintet).

***cis*-[Re₆Se₈(PET₃)₄(*t*-BuCN)₂](SbF₆)₂.** A solution of 89 mg (260 μmol) of AgSbF_6 in 2 mL of trimethylacetonitrile was added to a solution of 183 mg (74 μmol) of *cis*-[Re₆Se₈(PET₃)₄I₂]⁹ in 10 mL of dichloromethane. A yellow precipitate formed within seconds; the mixture was stirred with exclusion of light for 12 h and filtered. The filtrate was concentrated to an orange-red residue, which was redissolved in 5 mL of dichloromethane; the solution was stirred for 5 min and filtered through a plug of Celite. The filtrate was collected and concentrated *in vacuo* to near dryness. The residue was triturated with ether to give the product as 159 mg (75%) of an orange-red solid. ¹H NMR: δ 1.05 (q, Me), 1.12 (q, Me), 1.38 (s, *t*-Bu), 2.14 (q, CH₂), 2.25 (q, CH₂). ³¹P NMR: δ -18.0, -21.5. FAB-MS: m/z 2623 ($\text{M}^+ - \text{SbF}_6$).

***cis*-[Re₆Se₈(PET₃)₄(DMF)₂](SbF₆)₂.** A solution of 21 mg (61 μmol) of AgSbF_6 in 2 mL of DMF was added to a solution of 60 mg (24 μmol) of *cis*-[Re₆Se₈(PET₃)₄I₂] in 10 mL of dichloromethane. A yellow precipitate formed within seconds; the mixture was stirred with exclusion of light for 12 h and filtered. The filtrate was concentrated to an orange-red residue, which was redissolved in 5 mL of dichloromethane; the solution was stirred for 5 min and filtered through a plug of Celite. The filtrate was collected and concentrated *in vacuo* to near dryness. The residue was triturated with ether to give the

product as 60 mg (88%) of an orange-red solid. ¹H NMR: δ 1.05 (q, Me), 1.15 (q, Me), 2.12 (q, CH₂), 2.28 (q, CH₂), 2.86 (s, Me), 3.06 (s, Me), 8.30 (s, CH). ³¹P NMR: δ -17.7, -21.2. FAB-MS: m/z 2604 ($\text{M}^+ - \text{SbF}_6$).

***cis*-[Re₆Se₈(PET₃)₄(Me₂SO)₂](SbF₆)₂.** A solution of 18 mg (52 μmol) of AgSbF_6 in 2 mL of DMSO was added to a solution of 52 mg (21 μmol) of *cis*-[Re₆Se₈(PET₃)₄I₂] in 10 mL of dichloromethane. A yellow precipitate formed within seconds; the mixture was stirred with exclusion of light for 12 h and filtered. The filtrate was concentrated to an orange-red residue, which was redissolved in 5 mL of dichloromethane; the solution was stirred for 5 min and filtered through a plug of Celite. The filtrate was collected and concentrated *in vacuo* to near dryness. The residue was triturated with ether to give the product as 49 mg (81%) of an orange-red solid. ¹H NMR: δ 1.04 (q, Me), 1.15 (q, Me), 2.11 (q, CH₂), 2.27 (q, CH₂), 2.59 (s, Me). ³¹P NMR: δ -17.6, -21.1. FAB-MS: m/z 2535 ($\text{M}^+ - \text{SbF}_6 - \text{Me}_2\text{SO}$).

***cis*-[Re₆Se₈(PET₃)₄(py)₂](SbF₆)₂.** To a solution of 25 mg (9.0 μmol) of *cis*-[Re₆Se₈(PET₃)₄(MeCN)₂](SbF₆)₂⁹ in 5 mL of chlorobenzene was added 1 mL of pyridine (py). The mixture was stirred and refluxed for 4 d to give an ochre-colored solution. Ether (20 mL) was added to produce a brown precipitate. The precipitate was dissolved in 5 mL of dichloromethane; the solution was stirred for 5 min and filtered through a plug of Celite. The filtrate was collected and concentrated *in vacuo* to near dryness. The residue was triturated with ether to give the product as 20 mg (79%) of an orange-red solid. ¹H NMR: δ 1.05 (q, Me), 1.12 (q, Me), 2.18 (q, CH₂), 2.30 (q, CH₂), 7.32 (t, β -H), 8.00 (t, γ -H), 9.40 (d, α -H). ³¹P NMR: δ -19.2, -22.0. FAB-MS: m/z 2617 ($\text{M}^+ - \text{SbF}_6$).

***trans*-[Re₁₂Se₁₆(PET₃)₈(MeCN)₂](SbF₆)₄.** A Pyrex ampule (i.d. \times o.d. \times l = 8 \times 12 \times 150 mm) was charged with 30 mg (11 μmol) of *cis*-[Re₆Se₈(PET₃)₄(MeCN)₂](SbF₆)₂ and heated under dynamic vacuum in an oil bath. After 24 h at 180 $^\circ\text{C}$, a greenish-black solid was obtained. This material was dissolved in dichloromethane to give a dark green solution. Ether was introduced over 2 d by vapor diffusion, causing separation of the product as 20 mg (68%) of brown-green needles. ¹H NMR: δ 1.04–1.26 (m, Me), 2.24 (q, CH₂), 2.29 (q, CH₂), 2.37 (q, CH₂), 2.46 (q, CH₂), 2.76 (s, MeCN). ³¹P NMR: δ -10.6, -15.6, -18.2, -18.8. Electrospray-MS: m/z 1111 ($[\text{Re}_{12}\text{Se}_{16}(\text{PET}_3)_8]^{4+}$), 1132 ($[\text{Re}_{12}\text{Se}_{16}(\text{PET}_3)_8(\text{MeCN})_2]^{4+}$). This compound was further identified by an X-ray structure determination.

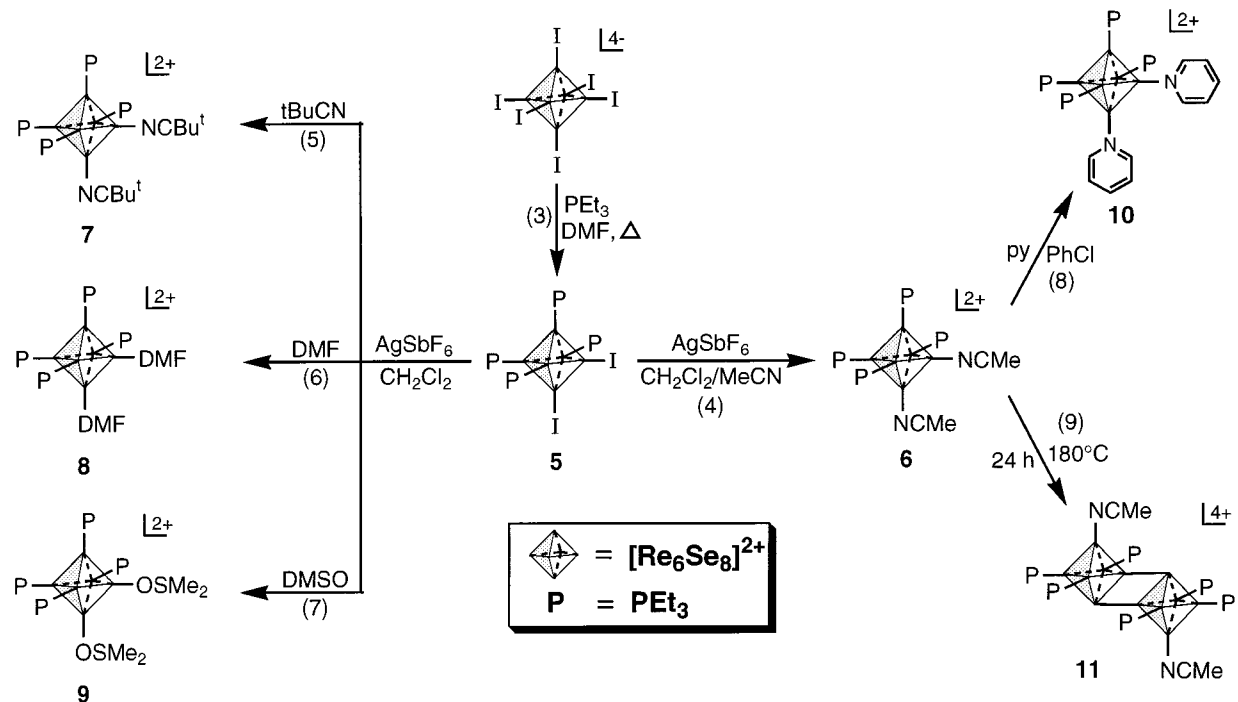


Figure 2. Substitution reactions of *cis*-[Re₆Se₈(PEt₃)₄I₂] (5) leading to solvent-ligated clusters 6–9 in reactions 4–7 and the formation of 10 and the dicluster 11 from [Re₆Se₈(PEt₃)₄(MeCN)₂]²⁺ (9). The depiction of 11 is highly schematic and meant to imply the formation of a Re₂Se₂ rhomb. Reactions 3 and 4 were previously reported.⁹

Designation of Clusters. The following clusters 5–12 are of particular interest in the present investigation; 5, 6, and 12 were previously reported.

<i>cis</i> -[Re ₆ Se ₈ (PEt ₃) ₄ I ₂]	5 ⁹
<i>cis</i> -[Re ₆ Se ₈ (PEt ₃) ₄ (MeCN) ₂] ²⁺	6 ⁹
<i>cis</i> -[Re ₆ Se ₈ (PEt ₃) ₄ (NCBu ^t) ₂] ²⁺	7
<i>cis</i> -[Re ₆ Se ₈ (PEt ₃) ₄ (DMF) ₂] ²⁺	8
<i>cis</i> -[Re ₆ Se ₈ (PEt ₃) ₄ (OSMe ₂) ₂] ²⁺	9
<i>cis</i> -[Re ₆ Se ₈ (PEt ₃) ₄ (py) ₂] ²⁺	10
<i>trans</i> -[Re ₁₂ Se ₁₆ (PEt ₃) ₈ (MeCN) ₂] ⁴⁺	11
[Re ₁₂ Se ₁₆ (PEt ₃) ₁₀] ⁴⁺	12 ⁹

X-ray Structure Determinations. Structures were determined for the two compounds in Table 1. Suitable crystals of [9](SbF₆)₂ (orange-red) and [11](SbF₆)₄·4CH₂Cl₂ (brownish-green) were grown at room temperature by vapor diffusion of ether into concentrated dichloromethane solutions. Crystals were coated with Apiezon L grease, attached to glass fibers, and transferred to a Nicolet P3 ([9](SbF₆)₂) or Siemens SMART diffractometer ([11](SbF₆)₄·4CH₂Cl₂). Lattice parameters were obtained from least-squares analysis of more than 30 carefully centered reflections. Neither crystal showed significant decay over the course of data collection. The raw intensity data were converted (including corrections for scan speed, background, and Lorentz and polarization effects) to structure amplitudes and their esd's using the program XDISK ([9](SbF₆)₂) or SAINT ([11](SbF₆)₄·4CH₂Cl₂). An empirical absorption correction was applied to each data set with XEMP. Space group assignments were based on systematic absences, *E* statistics, and successful refinements of the structures. Structures were solved by direct methods with the aid of successive difference Fourier maps and were refined against all data using the SHELXTL 5.0 program package. In both structures, the thermal parameters of the light atoms (*Z* < 8) were refined isotropically, while those for heavier atoms were refined anisotropically. In the structure of [11](SbF₆)₄·4CH₂Cl₂, one anion was constrained and refined as a rigid octahedron; one dichloromethane was treated as a rigid tetrahedron

Table 1. Crystal Data and Structure Refinement Details for *cis*-[Re₆Se₈(PEt₃)₄(DMSO)₂](SbF₆)₂ and *trans*-[Re₁₂Se₁₆(PEt₃)₈(MeCN)₂](SbF₆)₄·4CH₂Cl₂

	[9](SbF ₆) ₂	[11](SbF ₆) ₄ ·4CH ₂ Cl ₂
empirical formula	C ₂₈ H ₇₂ F ₁₂ O ₂ P ₄ S ₂ Sb ₂ · Re ₆ Se ₈	C ₅₄ H ₁₃₄ Cl ₈ F ₂₄ N ₂ P ₈ Sb ₄ · Re ₁₂ Se ₁₆
fw	2849.24	5783.67
space group	<i>P</i> $\bar{1}$	<i>P</i> $\bar{1}$
λ , Å	0.710 73	0.710 73
<i>Z</i>	2	1
<i>a</i> , Å	11.973(2)	14.7882(3)
<i>b</i> , Å	12.642(3)	15.2959(1)
<i>c</i> , Å	21.717(4)	16.0551(4)
α , deg	101.76(3)	76.00(1)
β , deg	104.66(3)	64.734(1)
γ , deg	92.24(3)	72.225(1)
<i>V</i> , Å ³	3099(1)	3101(1)
<i>d</i> _{calc} , g/cm ³	3.053	3.080
μ , mm ⁻¹	17.45	17.55
<i>T</i> , K	223	213
crystal size, mm ³	0.5 × 0.5 × 0.4	0.1 × 0.1 × 0.2
2 θ range, deg	3.3–45.0	2.8–45.0
<i>R</i> , ^a <i>wR</i> ^b	5.83, 13.41	8.20, 16.52

$$^a R = \sum(|F_o| - |F_c|) / \sum|F_o|. \quad ^b wR2 = [\sum w(|F_o| - |F_c|)^2 / \sum w|F_o|^2]^{1/2}.$$

with a fixed C–Cl distance of 1.78 Å. Hydrogen atoms were assigned to ideal positions and were refined using a riding model with an isotropic thermal parameter 1.2× that of the attached carbon atom (1.5× for methyl hydrogens). Crystallographic data are listed in Table 1.¹¹

Other Physical Measurements. NMR spectra were recorded on a Bruker AM 500 spectrometer. Chemical shifts of ³¹P spectra were referenced to 85% H₃PO₄ (negative values upfield). FAB mass spectra were determined using a JEOL SX-102 spectrometer with 3-nitrobenzyl alcohol as the matrix material. Electrospray mass spectra were recorded using a Platform 2 mass spectrometer (Micromass Instruments, Danvers, MA). Cyclic voltammetry was performed in acetonitrile solutions with a PAR Model 263 potentiostat/galvanostat using a Pt working electrode and 0.1 M (Bu₄N)(PF₆) as the supporting electrolyte; potentials are

(11) See paragraph at the end of this article concerning Supporting Information available.

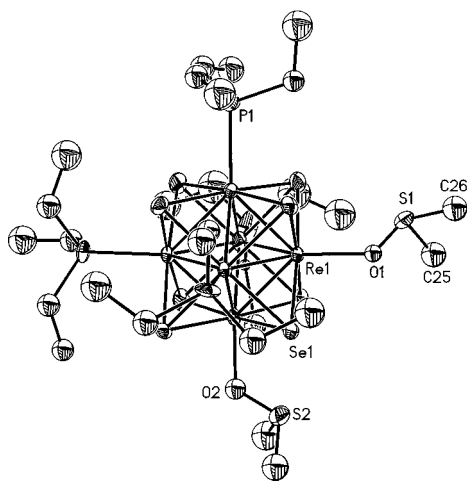


Figure 3. Structure of $cis\text{-}[\text{Re}_6\text{Se}_8(\text{PEt}_3)_4(\text{Me}_2\text{SO})_2]^{2+}$ as its SbF_6^- salt. 50% thermal ellipsoids and a partial atom-labeling scheme are shown.

referenced to the SCE. Thermal stabilities of clusters were investigated using a DuPont Model 2000 thermogravimetric analyzer.

Results and Discussion

Research on Re_6Q_8 clusters in this laboratory proceeds in several stages: (i) dimensional reduction of $\text{Re}_6\text{Q}_8\text{X}_2$ phases to afford crystalline solids containing the individual clusters $[\text{Re}_6\text{Q}_8\text{X}_6]^{4-}$ as soluble salts;^{6,7} (ii) substitution of terminal halide ligands of selected clusters with triethylphosphine to afford the series $[\text{Re}_6\text{Se}_8(\text{PEt}_3)_n\text{I}_{6-n}]^{(n-4)+}$ ($n = 3-6$)⁹ and $[\text{Re}_6\text{S}_8(\text{PEt}_3)_n\text{Br}_{6-n}]^{(n-4)+}$ ($n = 2-6$);¹⁰ (iii) substitution of halide with a relatively labile neutral ligand in order to investigate the possible formation of condensed diclusters and tetraclusters by the methods of Figure 1;⁹ (iv) formation of multicusters using bridging ligands terminal to individual cluster units. This investigation is part of stage iii; consequently, we are concerned with the synthesis and structures of *cis*-disubstituted clusters of general type **3**, of which only **6** had been previously prepared.

Monoclusters. Synthetic reactions 3–9 carried out in this work are summarized in Figure 2. The reaction scheme originates with the preparation of *cis*-diiodide cluster **5** by the previously reported reaction 3.⁹ In reaction 4, this cluster undergoes iodide substitution in the presence of $\text{Ag}(\text{I})$ to afford the bis(acetonitrile) cluster **6**. To provide additional examples of this cluster type and further proof of retention of stereochemistry upon substitution, reactions 5–8 were investigated. These afforded the indicated products **7–10** as SbF_6^- salts, characterized by NMR and FAB-MS, in yields of 75–88% as orange-red solids soluble in dichloromethane, acetonitrile, Me_2SO , and DMF. In particular, ³¹P NMR spectra were most useful for determining stereochemistry. Clusters **7–10** showed two equally intense signals in the range $\delta -17$ to -22 in acetonitrile solutions, consistent with core C_{2v} symmetry. The structure of **9** is set out in Figure 3, from which retention of *cis* stereochemistry is immediately apparent. Because cluster dimensions compare closely with those of other $[\text{Re}_6\text{Se}_8]^{2+}$ species,^{7,9} ranges and mean values, rather than individual metric data, are given in Table 2. The Re–P mean bond distance of 2.479(8) Å is indistinguishable from that of **6** (2.488(5) Å),⁹ implying comparable thermal stability. The Me_2SO ligands are O-bonded with Re–O bond lengths of 2.14(2) and 2.19(2) Å. These are comparable with the mean Re–O distance of 2.15 Å in $[\text{Re}_6\text{Se}_8(\text{OSMe}_2)_6]^{2+}$ ¹² but are much shorter than the only other two reported Re–OSR₂ bond lengths (2.30–2.35 Å)

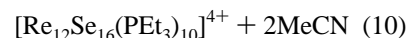
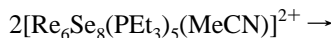
Table 2. Selected Interatomic Distances (Å) and Angles (deg) for $cis\text{-}[\text{Re}_6\text{Se}_8(\text{PEt}_3)_4(\text{DMSO})_2](\text{SbF}_6)_2$ and $trans\text{-}[\text{Re}_{12}\text{Se}_{16}(\text{PEt}_3)_8(\text{MeCN})_2](\text{SbF}_6)_4 \cdot 4\text{CH}_2\text{Cl}_2$

	[9] (SbF_6) ₂	[11] (SbF_6) ₄ ·4 CH_2Cl_2
Re–N		2.15(4)
Re–O	2.14(2)	
	2.19 (2)	
mean	2.17	
Re–P	2.467(7)	2.47(1)
	2.479(8)	2.48(1)
	2.481(8)	2.48(1)
	2.487(8)	2.50(1)
mean	2.479(8)	2.48(1)
Re–Re	2.615(2)–2.645(2)	2.612(2)–2.661(2)
mean	2.630(9)	2.63(1)
Re–Se ^a	2.506(3)–2.528(3)	2.508(4)–2.526(4)
mean	2.517(6)	2.516(5)
Re–Re–O	133.9(5)–135.8(4)	
mean	134.8(8)	
Re–Re–N		134.0(9)–135.8(9)
mean		135.0(8)
Re–Re–P	131.4(2)–138.5(2)	132.8(3)–137.8(3)
mean	135(2)	135.0(8)
Re–Re–Re ^b	59.5(1)–60.5(1)	59.20(6)–61.07(6)
mean	60.0(2)	60.0(4)
Re–Re–Re ^c	89.5(1)–90.6(1)	89.39(6)–90.84(7)
mean	90.0(3)	90.0(4)
Re–Re–Se	58.1(1)–58.9(1)	58.1(1)–61.7(1)
mean	58.5(2)	58.6(7)
Re–Se–Re ^a	62.3(1)–63.6(1)	60.9(1)–63.7(1)
mean	63.0(3)	63.0(7)
Se–Re–O	90.1(4)–92.6(4)	
mean	91.6(8)	
Se–Re–N		90.3(9)–92.6(9)
mean		91(1)
Se–Re–P	89.1(2)–94.7(2)	89.5(2)–94.7(3)
mean	92(2)	92(1)
Se–Re–Se ^a	89.3(1)–90.6(1)	86.3(1)–93.0(1)
mean	90.0(7)	90(1)
within Re_2Se_2 rhomb		
Re–Se		2.630(4)
		2.611(4)
mean		2.621
Re–Se–Re		80.4(1)
Se–Re–Se		99.6(1)

^a Excluding Re_2Se_2 rhomb. ^b Within triangular faces. ^c Within equatorial squares.

which, however, refer to terminal ligation in multiply bonded dinuclear complexes.¹³

Diclusters. (a) Formation. Reaction 9, examined in this work, and reaction 10, accomplished previously,⁹ are of immediate interest. Reaction 10 has only one rational outcome if



acetonitrile is preferentially expelled from the reactant cluster, the resultant species does not sustain coordinative unsaturation, and the counteranion (SbF_6^- , BF_4^-) is chemically inert. Given the formation of **12** in good yield, these aspects must intervene. We also observed at the outset another factor favorable to the formation of **12**. In the crystalline phase, pairs of the clusters $[\text{Re}_6\text{Se}_8(\text{PEt}_3)_5(\text{MeCN})]^{2+}$ are favorably aligned, with their

(12) Zheng, Z.; Holm, R. H. Results to be published.

(13) (a) Koz'min, P. A.; Surazhskaya, M. D.; Larina, T. B. *Koord. Khim.* **1979**, 5, 598. (b) Hursthouse, M. B.; Malik, K. M. A. *J. Chem. Soc., Dalton Trans.* **1979**, 409.

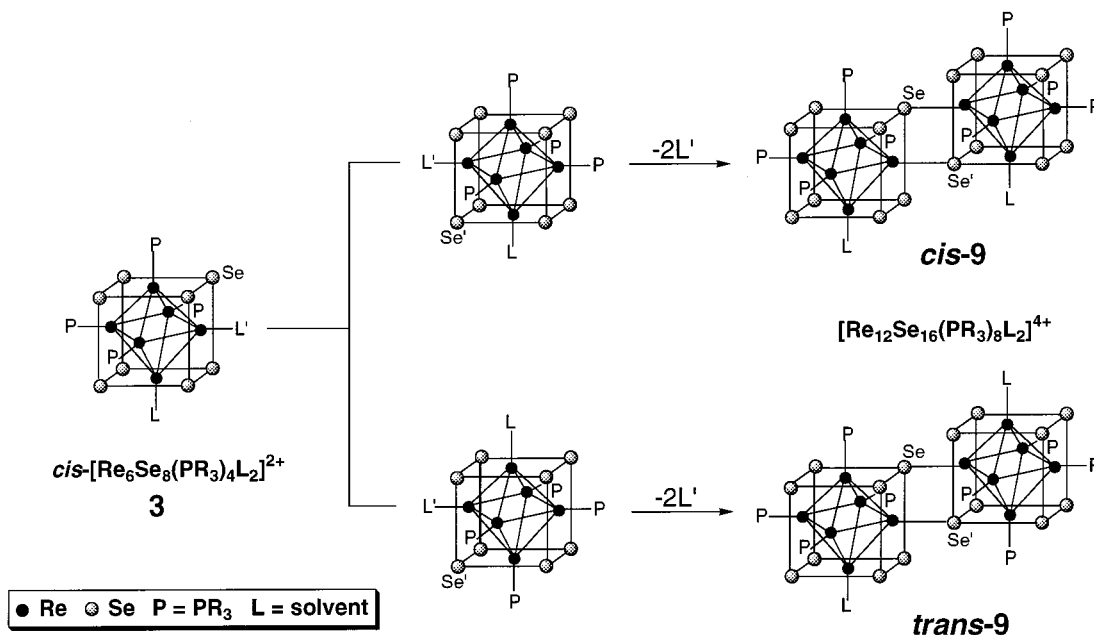


Figure 4. Schematic representation of the effects of the relative orientations of two *cis*-disubstituted monocusters **3** in the formation of isomers of a rhomb-linked dicluster **13** by thermolysis. The designated selenium atoms (Se, Se') are those involved in Re_2Se_2 rhomb formation upon elimination of labile ligands L' .

$\text{ReSe}_4(\text{MeCN})$ faces disposed toward each other across a $\text{Re}\cdots\text{Re}$ intercluster distance of 6.84 Å. Small translational and rotational movements of the clusters upon loss of acetonitrile orient the clusters for bridge rhomb formation. Because no other intercluster pairwise orientation is as favorable, we take the operation of this pathway as more probable than any other in this solid state reaction. While we cannot prove that it is essential to efficient dicluster formation, we assume that an analogous pathway in reaction 2 would promote the formation of tetracuster **4** (Figure 1). However, this reaction, while our best conception of a directed synthesis of the cyclic tetracuster, does not necessarily have an unambiguous outcome.

In Figure 4, the two possible culminations of the thermolysis of cluster **3** based on pairwise interaction of mono-deligated clusters are set out. In the upper pathway, the unsaturated clusters collapse to *cis*-**13**, while in the lower pathway the product is *trans*-**13**. The different isomers arise from different relative orientations of the clusters immediately before intercluster rhomb bridging (as shown) and/or from the formation of one intercluster $\text{Re}-\text{Se}$ bond with or without rotation about it preceding the second $\text{Re}-\text{Se}$ bond-making step. Given the robust nature of $\text{Re}-\text{Se}$ bonds, it is improbable that the two isomers can be interconverted at temperatures below that at which the remaining ligands L are removed. Consequently, only *cis*-**13** is viable in the formation of tetracuster **4**. Which dicluster is formed from **3** must be left to experiment, i.e., reaction 9.

Thermogravimetric examination of $[\text{Re}_6\text{Se}_8(\text{PET}_3)_5(\text{MeCN})]-(\text{SbF}_6)_2$ revealed that evolution of acetonitrile was complete at 230 °C and that substantial weight loss due to the removal of phosphine occurred in the 320–390 °C range. Similarly, for $[\mathbf{6}](\text{SbF}_6)_2$, acetonitrile was removed by 270 °C and the majority of phosphine by 390 °C. In order to minimize any possible thermal decomposition of product clusters, cluster formation was conducted under somewhat milder conditions in dynamic vacuum. In this work, thermolysis reaction 9 has been examined at 180 °C for 24 h. Previously, we demonstrated the occurrence of the related reaction 10 under the same conditions. This reaction afforded a 94% isolated yield of fully phosphine-substituted dicluster **12** as the brown-green crystalline SbF_6^-

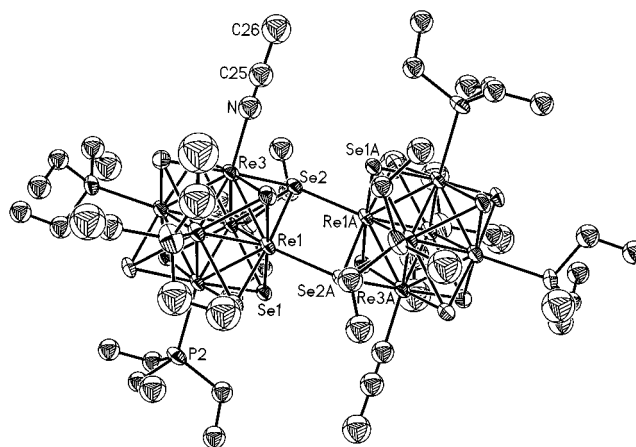


Figure 5. Structure of *trans*- $[\text{Re}_{12}\text{Se}_{16}(\text{PET}_3)_8(\text{MeCN})_2]^{4+}$ as its SbF_6^- salt. 50% thermal ellipsoids and a partial atom-labeling scheme are shown. Atoms n and nA are related by an inversion center.

salt. In the case of reaction 9, which was carried out in multiple experiments, the product cluster revealed four equally intense ^{31}P resonances in the range $\delta -10$ to -19 , consistent with a dicluster having an inversion center or C_2 axis or with a centrosymmetric dicluster **4**. The matter was resolved by an X-ray structure determination; the best crystals available for the structural study were of only moderate diffraction quality. The reaction product was revealed to be the dicluster compound **[11]**- $(\text{SbF}_6)_4$, obtained in 68% yield as brown-green crystals.

(b) Structure. The structure of dicluster **11**, with imposed centrosymmetry, is shown in Figure 5. The overall core structure is essentially congruent with that of **12**.⁹ Ranges and mean values of core bond distances and angles and $\text{Re}-\text{P}$ bond lengths are indistinguishable. Two structural features are of added significance. The reactant clusters are now connected by the rhomb $\text{Re}_2(1,1A)\text{Se}_2(2,2A)$. The rhomb is planar with slightly unequal $\text{Re}-(\mu_4\text{-Se})$ bond lengths whose mean value (2.621 Å) is, as expected, much longer than that of the core $\text{Re}-(\mu_3\text{-Se})$ distances (2.516(5) Å) because of the difference in bridge multiplicity. The two acetonitrile ligands retained in reaction 9 are located in a *trans* orientation at the $\text{Re}(3)$ and

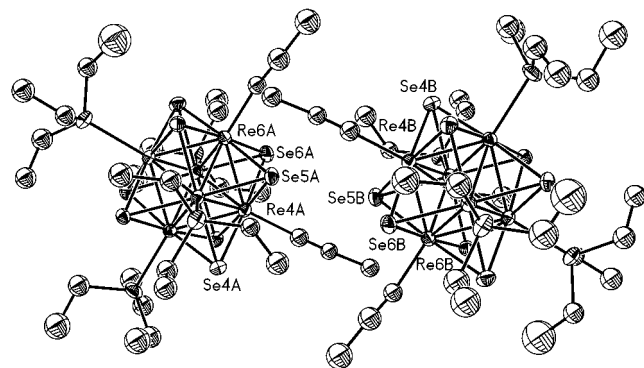


Figure 6. Orientation of adjacent clusters (A,B) in the crystal structure of *cis*-[Re₆Se₈(PET₃)₄(MeCN)₂](SbF₆)₂.⁹ The clusters are related by an inversion center. Selected intercluster distances (Å): Re(4A)⋯Re(4B), 7.05; Re(4A)⋯Se(5B), 4.95; Re(4A)⋯Se(6B), 7.42; Re(4A)⋯Se(4B), 7.63; Re(6A)⋯Se(5B), 5.64; Re(6A)⋯Se(4B), 7.23; Re(6A)⋯Se(6B), 7.89.

Re(3A) sites, i.e., on opposite sides of the rhomb plane. Thus, the cluster has the *trans*-**13** configuration (Figure 4). The Re–N bond distances (2.15(4) Å) are not significantly different from those in [Re₆Se₈(PET₃)₅(MeCN)]²⁺ (2.15(1) Å) and **6** (mean 2.12 Å).⁹ The picture that emerges from reactions 9 and 10 is the thermal condensation of two face-capped cubic clusters to form diclusters whose individual cluster units are bridged by Re₂Se₂ rhombs and are not importantly different dimensionally from the starting clusters. Rhomb linkages between clusters are well recognized in Re–Q–X phases,^{2–6} and molecular examples, in addition to **11** and **12**, are increasing.^{9,14} Those most similar structurally to the present clusters are [Co₁₂S₁₆(PET₃)₁₀]²⁺¹⁵ and [Cr₁₂S₁₆(PET₃)₁₀],¹⁶ in which two [M₆(μ₃-Q)₈]^{1+/0} cores are linked by an M₂S₂ rhomb.

(c) Solid State Orientation Effects. The orientation of two adjacent clusters in the crystal structure of [**6**](SbF₆)₂⁹ is depicted in Figure 6. The two clusters are related by an inversion center. The symmetry-related core fragments Re(4A)Se₄(MeCN) and Re(4B)Se₄(MeCN) face each other across the intercluster distance Re(4A)⋯Re(4B) = 7.05 Å. The four selenide atoms of each fragment deviate from their mean plane by ±0.007 Å, and the Re atoms lie above these planes by 0.074 Å, in the direction of the acetonitrile ligands. The two Se₄ mean planes are exactly parallel. The arrangement for dicluster formation is no less favorable than for **12**. In the least-motion pathway, the distances Re(4A)⋯Se(5B) = Re(4B)⋯Se(5A) = 4.95 Å implicate these atoms in rhomb formation upon departure of the two acetonitrile ligands. The separations Re(4A)⋯Se(3B, 4B, 6B) are in the range 7.42–9.41 Å. If rhomb formation involving Re(4B) and Re(6A) were considered, the closest distance is Re(6A)⋯Se(5B), at 5.64 Å. The separations Re(6A)⋯Se(3B, 4B, 6B) are much longer (7.23–9.09 Å). While we cannot know whether the two acetonitrile ligands at Re(4A, 4B) are released first, that event together with the least-motion pathway necessarily leads to the *trans* isomer of **11**, as observed.

(d) Redox Capacity. Clusters containing the [Re₆Se₈]²⁺ core are electron-precise (24e⁻) and, consequently, do not possess an extensive redox chemistry, at least with halide, phosphine, and solvent ligands. Oxidations are observed at rather positive potentials. Thus, cluster **6** is oxidized in a chemically reversible

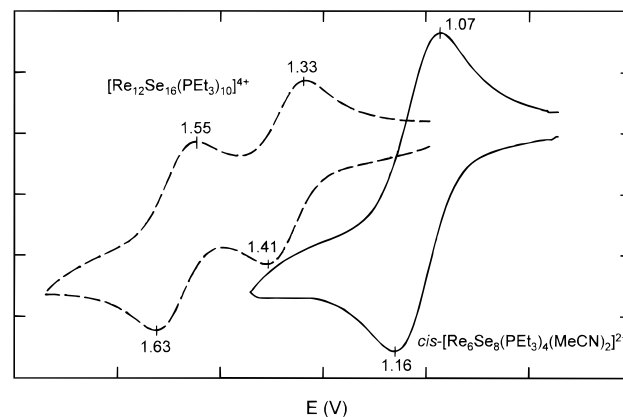


Figure 7. Cyclic voltammograms (50 mV/s) of monocluster *cis*-[Re₆Se₈(PET₃)₄(MeCN)₂]²⁺ ($E_{1/2} = 1.11$ V) and dicluster [Re₁₂Se₁₆(PET₃)₁₀]⁴⁺ ($E_{1/2} = 1.37, 1.59$ V) in acetonitrile solutions. Peak potentials are indicated.

($i_{pa}/i_{pc} \approx 1$) one-electron process at $E_{1/2} = 1.12$ V in acetonitrile. Dicluster **12** exhibits *two* redox steps in the same solvent, at $E_{1/2} = 1.37$ and 1.59 V. Voltammograms of the two clusters are provided in Figure 7. The two redox steps of **12** are coupled by virtue of the intimate contact of individual cluster units through the rhomb interaction. Indeed, [Cr₁₂S₁₆(PET₃)₁₀] exhibits a related behavior, evidencing two oxidations separated by 440 mV. Inasmuch as [Cr₆S₈(PET₃)₆] can also be reduced, the dicluster develops two reduction steps separated by 550 mV.¹⁶ The larger separations must arise from a more intimate interaction between individual cluster units which could be primarily structural in nature. We note that the metal–metal distance in the bridging rhomb of [Cr₁₂S₁₆(PET₃)₁₀] (2.95 Å)¹⁶ is considerably shorter than that in **12** (3.42 Å).

Summary. The *cis*-substituted bis(acetonitrile) cluster **6** is a useful precursor by thermolysis to the new *trans* dicluster **11**, one of only four molecular clusters^{9,15,16} that contain the rhomb-bridged core [M₁₂(μ₃-Q)₁₄(μ₄-Q)₂]^z of idealized centrosymmetry. Conversion to the cyclic tetracluster **4** by thermolysis (Figure 1) requires as an intermediate a dicluster of the type *cis*-**13** (Figure 4). Consequently, the directed synthesis of the tetracluster reduces to the preparation of a suitable *cis* dicluster. This in turn may require a precursor cluster compound whose solid state structure is such that, under the least-motion concept in thermolysis, formation of *trans*-**13** is not favored. If the solid state structure of the initial *cis*-disubstituted monocluster is irrelevant, formation of both the *cis* and *trans* isomers of the dicluster is expected as a consequence of rotation about the initially formed Re–Se bond. Such isomers, as are those of monoclusters,^{9,10} should be separable. If rotation is restricted, the situation becomes one in which relative orientations of unsaturated clusters presumably dictate the stereochemistry of the dicluster. These matters are under continuing investigation.

Acknowledgment. This research was supported by a grant from Nycomed, Inc., and by NSF Grant 94-23830. X-ray diffraction equipment was obtained with NIH Grant 1 S10 RR 02247. We thank Dr. J. R. Long for valuable discussions and F. Deng for assistance with thermogravimetric measurements and the use of equipment.

Supporting Information Available: X-ray structural information for the compounds in Table 1, including tables of crystal and intensity collection data, positional and thermal parameters, and interatomic distances and angles (27 pages). Ordering information is given on any current masthead page.

(14) Harmjan, M.; Saak, W.; Haase, D.; Pohl, S. *J. Chem. Soc., Chem. Commun.* **1997**, 951.

(15) Cecconi, F.; Ghilardi, C. A.; Midollini, S.; Orlandini, A. *Inorg. Chim. Acta* **1993**, *214*, 13.

(16) Kamiguchi, S.; Imoto, H.; Saito, T. *Chem. Lett.* **1996**, 555.